

Maximizing Discrimination Capability of Knowledge Distillation with Energy-based Score

Seonghak Kim^{a,*}, Gyeongdo Ham^{a,*}, Suin Lee^a, Donggon Jang^a, Daeshik Kim^{a,**}

^a*School of Electrical Engineering, Korea Advanced Institute of Science and Technology, 291, Daehak-ro, Yuseong-gu, Daejeon, 34141, Republic of Korea*

Abstract

To apply the latest computer vision techniques that require a large computational cost in real industrial applications, knowledge distillation methods (KDs) are essential. Existing logit-based KDs apply the constant temperature scaling to all samples in dataset, limiting the utilization of knowledge inherent in each sample individually. In our approach, we classify the dataset into two categories (i.e., low energy and high energy samples) based on their energy score. Through experiments, we have confirmed that low energy samples exhibit high confidence scores, indicating certain predictions, while high energy samples yield low confidence scores, meaning uncertain predictions. To distill optimal knowledge by adjusting non-target class predictions, we apply a higher temperature to low energy samples to create smoother distributions and a lower temperature to high energy samples to achieve sharper distributions. When compared to previous logit-based and feature-based methods, our energy-based KD (Energy KD) achieves better performance on various datasets. Especially, Energy KD shows significant improvements on CIFAR-100-LT and ImageNet datasets, which contain many challenging samples. Furthermore, we propose high energy-based data augmentation (HE-DA) for further improving the performance. We demonstrate that meaningful perfor-

*Authors contributed equally

**Corresponding author

This work has been submitted to the Elsevier for possible publication. Copyright may be transferred without notice, after which this version may no longer be accessible.

Email addresses: hakk35@kaist.ac.kr (Seonghak Kim), rudeh6185@kaist.ac.kr (Gyeongdo Ham), suinlee@kaist.ac.kr (Suin Lee), jdg900@kaist.ac.kr (Donggon Jang), daeshik@kaist.ac.kr (Daeshik Kim)

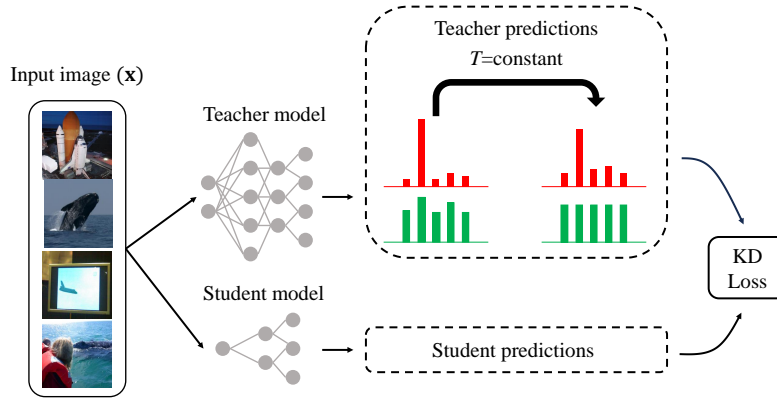
mance improvement could be achieved by augmenting only 20-50% of dataset, suggesting that it can be employed on resource-limited devices. To the best of our knowledge, this paper represents the first attempt to make use of energy scores in KD and DA, and we believe it will greatly contribute to future research.

Keywords: Knowledge distillation, Energy score, Temperature adjustment, Data augmentation, Resource-limited device

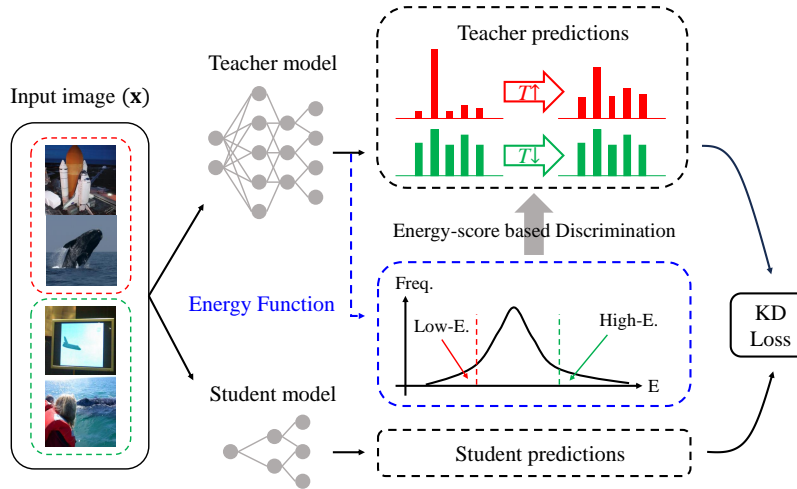
1. Introduction

In the past few years, there have been significant advancements in the field of computer vision, such as image classification (He et al. (2016a); Ma et al. (2018a)), object detection (Ren et al. (2015); He et al. (2017)), and image segmentation (Zhao et al. (2017); Long et al. (2015)), due to the advent of deep learning. However, these deep learning-based models have become huge to ensure high performance, resulting in substantial computational costs, which makes it challenging to apply them in real-world industries. To overcome the limitations, model compression methods, such as model pruning (Liu et al. (2021)), quantization (Zhou et al. (2018)), and knowledge distillation (KD) (Gou et al. (2021)), have been proposed. Among these, KD has been widely applied in many fields of computer vision due to its higher performance and ease of implementation compared to other methods. KD involves training a lightweight student model by receiving meaningful information from a heavy teacher model, enabling the student model to achieve performance similar to that of the teacher model.

Since its introduction by Hinton et al. (2015), KD has evolved into two main approaches: logits-based (Zhao et al. (2022)) and features-based distillation (Chen et al. (2021a)). To train the student using information from the teacher, the logits-based methods utilize final predictions, while features-based methods leverage information from intermediate layers. Although it is generally known that features-based methods outperform logits-based methods, they can be challenging to use because, in some real-world applications, access to the intermediate layers of the teacher model may not be possible due to privacy and safety concerns. For this reason, this paper focuses on logits-based distillation, which does not require accessing the features of intermediate layers and thus offers practical advantages for real-world applications.



(a) Knowledge distillation with constant temperature scaling



(b) Knowledge distillation with different temperature scaling based on the energy scores

Figure 1: Schematic diagram of conventional knowledge distillation and our method: (a) constant temperature scaling, (b) different temperature scaling. Our method receives the energy score of each sample from the blue dashed line.

To mitigate the performance gap between the student and teacher models, we propose a new logit-based distillation method that is effective and easy to apply. As shown in Figure 1, we distinguish the entire dataset into low energy and high energy samples based on the energy scores of each sample. Then, we apply different temperature scaling to the separated samples (i.e., high temperature to low energy and low temperature to high energy samples). This allows us to obtain smoother distributions from low energy samples and sharper distributions from high energy samples, thereby adjusting non-target class predictions for optimal knowledge distillation. As a result, our methods significantly enhance the performance of the student model.

Additionally, we propose the high energy-based data augmentation (HE-DA) to further enhance the performance. In previous augmentation-based KD methods, DA is applied to the entire dataset, requiring more storage and computational cost. However, Our HE-DA achieved similar or even better performance, although utilizing only 20% to 50% of the dataset, which offers practical advantages. Through extensive experimentation on commonly used classification task datasets, such as CIFAR-100 (Krizhevsky et al. (2009)) and ImageNet (Russakovsky et al. (2015)), we have verified that our proposed methods outperform existing state-of-art approaches, particularly demonstrating strengths in the case of challenging datasets, such as CIFAR-100-LT and ImageNet.

2. Related Works

2.1. Knowledge Distillation

Knowledge distillation (KD) is a technique used to improve the performance of lightweight student networks through the "dark knowledge" of large teacher networks. In the past years, KD methods have evolved to narrow the performance gap between the student model and the teacher model by utilizing the model's final predictions (Cho and Hariharan (2019); Furlanello et al. (2018); Mirzadeh et al. (2020); Yang et al. (2019); Zhang et al. (2018)) and intermediate features (Heo et al. (2019a,c); Huang and Wang (2017); Kim et al. (2018); Park et al. (2019a)). Chen et al. (2021b) applied a review mechanism to leverage past features for guiding the current ones using residual learning. Furthermore, they introduced an attention-based fusion (ABF) and a hierarchical context loss (HCL) to further enhance performance. Zhao et al. (2022) separated soft-label distillation loss into two distinct components: target class knowledge distillation (TCKD) and non-target class knowledge distillation

(NCKD). This separation allowed each part to independently harness its effectiveness. These approaches prioritize effective knowledge transfer, but do not address the concept of differentiating energy for a particular sample and the methodology for discriminating and transferring knowledge from that sample. Our approach brings a fresh perspective to KD by suggesting that knowledge transfer should be regulated according to an energy-based score. This approach further improves performance when dealing with noise samples, indicating that the proposed method is more suitable for real-world applications. Our energy-based KD (Energy KD) is an important step forward in developing more effective and efficient KD techniques.

2.2. Energy-based Learning

Energy-based machine learning models have a long history, starting with the Boltzmann machine (Ackley et al. (1985); Salakhutdinov and Larochelle (2010)), which is a network of units with associated energy for the entire network. Energy-based learning (LeCun et al. (2006); Ranzato et al. (2006, 2007)) provides a unified framework for various probabilistic and non-probabilistic learning approaches. Recent research (Zhao et al. (2016)) demonstrated the use of energy functions to train generative adversarial networks (GANs), where the discriminator utilizes energy values to differentiate between real and generated images. Xie et al. (2018a,b, 2019) also established the connection between discriminative neural networks and generative random field models. Subsequent studies have explored the application of energy-based models in video generation and 3D geometric patterns. Liu et al. (2020a) demonstrated that non-probabilistic energy scores can be directly used in a score function for estimating out-of-distribution (OOD) uncertainty. They show that these optimization goals fit more naturally into an energy-based model than a generative model and enable the exploitation of modern discriminative neural architectures. Building upon these prior works, our proposed framework extends the use of non-probabilistic energy values to knowledge distillation (KD). Notably, our KD framework provides different knowledge for low energy and high energy samples, representing a novel contribution.

3. Methods

3.1. Background

Our approach revolves around categorizing each sample in the dataset into two groups: low energy and high energy. these groups are determined by the energy level, which maps the input \mathbf{x} to a single, non-probabilistic scalar value (i.e., $E(\mathbf{x}) : \mathbb{R}^d \rightarrow \mathbb{R}$) (LeCun et al. (2006)). The representation of the energy function is as described as follows:

$$E(\mathbf{x}; f) = -T^E \cdot \log \sum_1^K e^{f_i(\mathbf{x})/T^E}, \quad (1)$$

where $f_i(\mathbf{x})$ indicates the logit corresponding to the i^{th} class label, T^E is the temperature parameter for energy score, and K denotes total number of classes.

The motivation behind segregating categories according to energy scores is that we can regard input data with low likelihood as high energy samples (Liu et al. (2020b)). This can be achieved by utilizing the data’s density function $p(\mathbf{x})$ expressed by the energy-based model (LeCun et al. (2006); Grathwohl et al. (2019)).

$$p(\mathbf{x}) = \frac{e^{-E(\mathbf{x};f)/T^E}}{\int_{\mathbf{x}} e^{-E(\mathbf{x};f)/T^E}}, \quad (2)$$

where the denominator can be disregarded since it remains constant independently. Therefore, it can be expressed by

$$\log p(\mathbf{x}) = -\frac{E(\mathbf{x}; f)}{T^E} - C. \quad (3)$$

This equation shows that the energy function is proportional to the log likelihood function. In other words, samples with lower energy have a higher probability of occurrence, indicating a ‘certain image’, while samples with higher energy have a lower probability of occurrence, referring a ‘uncertain image’. This distinguishable nature of the energy function can be effectively utilized to categorizes samples, thereby facilitating optimal knowledge distillation. In order to observe the relationship between energy scores and images, Figure 3 in Section 4 displays images characterized by low and high energy, respectively. For a more comprehensive explanation, please refer to Section 4.

Consequently, the energy score, being a valuable tool for dataset division, can be employed in both knowledge distillation (KD) and data augmentation (DA) separately. Further elaboration on each method will be provided in the subsequent sections.

3.2. EnergyKD: Energy-based Knowledge Distillation

Using mentioned energy score, we propose a unified framework, energy-based knowledge distillation (Energy KD) method, where the differences between low and high energy allow effective transfer of knowledge. We obtain energy scores from pre-trained teacher models, using them to adjust the softmax temperature scaling for optimal distillation. This ensures that the teacher model possesses a distribution with adequate dark knowledge.

KD methods start by obtaining the knowledge from teacher and student models as follows:

$$\mathcal{T} = f_{\mathcal{T}}(\mathbf{x}; \theta_{\mathcal{T}}) \quad (4)$$

$$\mathcal{S} = f_{\mathcal{S}}(\mathbf{x}; \theta_{\mathcal{S}}), \quad (5)$$

where \mathbf{x} corresponds to the input image, $f_{\mathcal{T}}$ and $f_{\mathcal{S}}$ represent the teacher and the student model, respectively, and $\theta_{\mathcal{T}}$ and $\theta_{\mathcal{S}}$ are parameters of each model. We calculate the energy scores from teacher model, which are explained by

$$\mathcal{T}^E = E(\mathbf{x}; \mathcal{T}). \quad (6)$$

We sort the input images by these energy scores: the lower energy value, the more it falls into the certain group, and the higher energy value, the more it falls into the uncertain group.

For conventional KD loss, the Kullback-Leibler (KL)-divergence loss is used as follows:

$$\mathcal{L}_{KD}(\mathbf{x}; \mathcal{S}, \mathcal{T}, T) = D_{KL}\left(\sigma\left(\frac{\mathcal{T}}{T}\right) \parallel \sigma\left(\frac{\mathcal{S}}{T}\right)\right), \quad (7)$$

where σ is the softmax function and T is the temperature scaling factor.

On the other hand, the our method has the effect of adaptively adjusting the confidence based on the energy score level, which can be utilized by simply changing the temperature scaling factor ($T \rightarrow T_{\text{ours}}$):

$$\mathcal{L}_{\text{ours}}(\mathbf{x}; \mathcal{S}, \mathcal{T}, T_{\text{ours}}) = D_{KL}\left(\sigma\left(\frac{\mathcal{T}}{T_{\text{ours}}}\right) \parallel \sigma\left(\frac{\mathcal{S}}{T_{\text{ours}}}\right)\right) \quad (8)$$

$$T_{\text{ours}} = \begin{cases} T + T_{(-)}, & \mathcal{T}_i^E > \mathcal{T}_{\text{high}}^E = \mathcal{T}^E[N \cdot (1 - r)] \\ T + T_{(+)}, & \mathcal{T}_i^E \leq \mathcal{T}_{\text{low}}^E = \mathcal{T}^E[N \cdot r] \\ T, & \text{else} \end{cases}, \quad (9)$$

where $\mathcal{T}_{\text{high}}^E$ and $\mathcal{T}_{\text{low}}^E$ are the constant values to determine the range of high and low energy with rate ($r=\{0.2, 0.3, 0.4, 0.5\}$). $T_{(-)}$ has a negative integer to decrease the temperature and $T_{(+)}$ has a positive integer to increase the temperature. N denotes the number of samples and $[\cdot]$ means the index of array.

Previous research indicated that in order to enhance the performance of the KD, the dark knowledge must be appropriately distributed (Li et al. (2022)). Our approach can increase important "dark knowledge" about non-target classes in the low energy sample while increasing prediction of target-class in the high energy sample.

3.3. HE-DA: High Energy-based Data Augmentation

Our method achieves enhanced performance by incorporating data augmentation (DA) based on the energy scores. In conventional knowledge distillation (KD), DA is commonly applied to the entire dataset to enhance performance. However, this approach can be inefficient as it requires high computational cost. In our method, we leverage the energy scores to selectively augment specific samples, leading to comparable or even superior results compared to augmenting the entire dataset. Notably, we utilize only 20% to 50% of the dataset, demonstrating that favorable outcomes can be attained with less data, thereby optimizing computational cost.

In our energy KD approach, we sorted the energy scores obtained from the teacher model in ascending order. The lower values were categorized as being part of the low energy within the dataset, while the higher values were classified as belonging to the high energy. The entire datasets can be divided as follows:

$$\mathbf{x} = \{\mathbf{x}_{\text{low}}, \mathbf{x}_{\text{others}}, \mathbf{x}_{\text{high}}\} \quad (10)$$

$$\mathbf{x}_i = \begin{cases} \mathbf{x}_{\text{high}}, & \mathcal{T}_i^E > \mathcal{T}_{\text{high}}^E = \mathcal{T}^E[N \cdot (1 - r)] \\ \mathbf{x}_{\text{low}}, & \mathcal{T}_i^E \leq \mathcal{T}_{\text{low}}^E = \mathcal{T}^E[N \cdot r] \end{cases}, \quad (11)$$

where $\mathcal{T}_{\text{high}}^E$ and $\mathcal{T}_{\text{low}}^E$ are constant values to determine the size of high and low energy samples. We exclusively applied augmentation to samples that were classified as part of the high energy as follows:

$$\mathbf{x}_{\text{high}}^{\text{aug}} = G_{\text{aug}}(\mathbf{x}_{\text{high}}), \quad (12)$$

where G_{aug} refers the data augmentation function, here, we applied CutMix (Yun et al. (2019)) and MixUp (Zhang et al. (2017)). The results with MixUp are included in appendix.

Interestingly, our approach demonstrates higher performance compared to applying data augmentation solely to samples belonging to the low energy or applying it to both types of samples. We intend to validate this through subsequent experimental studies.

4. Experiments

The performance of the proposed method is evaluated in comparison to other knowledge distillation methods such as KD (Hinton et al. (2015)), AT (Zagoruyko and Komodakis (2016a)), OFD (Heo et al. (2019b)), CRD (Tian et al. (2019)), FitNet (Romero et al. (2014)), PKD (Park et al. (2019b)), RKD (Park et al. (2019b)), VID (Ahn et al. (2019)), DKD (Zhao et al. (2022)), ReviewKD (Chen et al. (2021a)), considering various architectural configurations including ResNet (He et al. (2016b)), WideResNet (Zagoruyko and Komodakis (2016b)), MobileNet (Sandler et al. (2018)), and ShuffleNet (Ma et al. (2018b)). Implementation details are presented in appendix. It is worth noting that **All experiments were repeated three times, and the reported results are the average values obtained.**

4.1. Datasets

CIFAR-100 (Krizhevsky et al. (2009)) is a widely accessible dataset frequently employed for image classification tasks. It comprises 100 classes, with samples having a resolution of 32×32 pixels. The dataset encompasses 50,000 images in the training set and 10,000 images in the test set.

ImageNet (Russakovsky et al. (2015)) is a comprehensive dataset extensively utilized for image classification tasks. It encompasses 1,000 classes,

and the samples within this dataset have dimensions of 224×224 pixels. The training set is incredibly large, containing 1.28 million images, while the test set consists of 5,000 images.

4.2. Effect of EnergyKD

Teacher	WRN-40-2	ResNet-56	ResNet-32x4	VGG 13	VGG 13	ResNet-32x4
Acc.	75.61	72.34	79.42	74.64	74.64	79.42
Student	WRN-16-2	ResNet-20	ResNet-8x4	VGG 8	MobileNetV2	ShuffleNetV2
Acc.	73.26	69.06	72.50	70.36	64.60	71.82
KD	<u>74.92</u>	<u>70.66</u>	73.33	<u>72.98</u>	<u>67.37</u>	74.45
FitNet	73.58	69.21	73.5	71.02	64.14	73.54
PKT	74.54	70.34	<u>73.64</u>	72.88	67.13	<u>74.69</u>
RKD	73.35	69.61	71.9	71.48	64.52	73.21
AT	74.08	70.55	73.44	71.43	59.40	72.73
VID	74.11	70.38	73.09	71.23	65.56	73.40
Energy KD	75.45	71.30	74.60	73.73	68.65	75.87
Δ	+0.53	+0.64	+0.96	+0.75	+1.28	+1.18

Table 1: Top-1 accuracy (%) on the CIFAR-100 test sets when using teacher and student models with the same and different architectures. The best results are highlighted in **bold** and the second best underlined. Δ means the performance gap between the best result and second best one.

Table 1 demonstrates that our method achieves higher performance on CIFAR-100 compared to the previous logit distillation approach. When applying our method to vanilla KD, we observed performance improvements ranging from 0.5 to 1.3 compared to the baseline. Furthermore, even when compared to other feature distillation methods, our method showcased remarkable performance improvements.

Additionally, when integrating our method into the recently developed logit distillation method (DKD) by simply adding the energy KD loss to the DKD loss. We observed performance enhancements in shown in Table 2. It is worth noting that our method had a greater impact on heterogeneous models compared to homogeneous models, indicating its scalability. These results imply that our method has the potential to be easily incorporated into future logit distillation methods.

ImageNet dataset results using Energy DKD are shown in the Table 3. The results demonstrate that our framework, Energy DKD, achieved significant improvement compared to other distillation methods. This is because we further optimized the knowledge distillation by applying different temperatures for low energy and high energy samples based on their energy score.

DKD	E	VGG13-8	VGG13-MV2	Res32x4-SV2
✓		74.68	69.71	77.07
✓	✓	75.21	70.49	77.71
		+0.53	+0.78	+0.64

Table 2: Scalability of our energy method. Integrating energy scores and DKD resulted in superior accuracy on CIFAR-100 datasets.

Distillation			Features				Logits		
R50-MV1	Teacher	Student	AT	OFD	CRD	ReviewKD	KD	DKD	Energy DKD
top-1	76.16	68.87	69.56	71.25	71.37	72.56	68.58	72.05	72.98
top-5	92.86	88.76	89.33	90.34	90.41	91.00	88.98	91.05	91.31
R34-R18	Teacher	Student	AT	OFD	CRD	ReviewKD	KD	DKD	Energy DKD
top-1	73.31	69.75	70.69	70.81	71.17	71.61	70.66	71.70	72.21
top-5	91.42	89.07	90.01	89.98	90.13	90.51	89.88	90.41	90.81

Table 3: Top-1 and Top-5 accuracy (%) on the ImageNet validation. In the row above, ResNet-50 is the teacher and MobileNet-V1 is the student. In the row below, ResNet-34 is the teacher and ResNet-18 is the student.

Based on the Top-1 accuracy, Energy DKD obtained performance gains of up to 0.6% over ReviewKD and up to 0.93% over DKD. The detailed hyperparameter settings and the effectiveness of each method are shown in appendix.

4.3. Temperature Ablations

Previously, we applied different temperatures to the low energy and high energy samples. To assess the validity of employing temperature scaling for both energy samples, we carried out temperature ablations for each samples, as presented in Table 4. Adjusting the temperature for samples in both ranges yielded superior results compared to exclusively modifying the temperature for either low energy or high energy samples. Moreover, we will extend our approach by applying several temperatures linked to energy scores across the entire dataset, alias Temperature Gradation, and then compare it to the method of treating only the two extremes. We partitioned the total dataset of CIFAR-100 into 10 segments based on their energy values, and then applied different temperatures to each segment. Specifically,

Teacher Student	ResNet32x4 ResNet8x4	ResNet32x4 ShuffleNetV2	Teacher Student	WRN-40-2 WRN-16-2	ResNet32x4 ResNet8x4	VGG 13 MobileNetV2	ResNet32x4 ShuffleNetV2
Low-	73.27	75.38	KD	75.06	73.33	67.37	74.45
High-	73.88	75.34	Gradation	75.49	74.32	68.57	75.74
Ours	74.60	75.87	Ours	75.45	74.60	68.65	75.87

Table 4: Left: Performance evaluated based on the sample type. 'Low-' indicates the application of temperature scaling only to low energy samples (i.e., high T), while 'High-' signifies the utilization of temperature scaling solely for high energy samples (i.e., low T)., Right: Comparing the effectiveness of temperature gradation with the temperature utilized in the performance analysis of our approach.

$$\mathbf{x} = \begin{cases} \mathbf{x}_1 \rightarrow T_1 = T_{\min} \\ \mathbf{x}_2 \rightarrow T_2 \\ \vdots \\ \mathbf{x}_n \rightarrow T_n \\ \vdots \\ \mathbf{x}_{10} \rightarrow T_{10} = T_{\max} \end{cases} \quad (13)$$

Table 4 reveals that the method which solely employed different temperatures for the two extremes achieved comparable performance, despite the Temperature Gradation method applying a broader range of temperature scaling. Based on this experiment, we draw the conclusion that prioritizing the handling of certain and uncertain images is more crucial than dealing with intermediate images. The detailed information regarding each experiment can be found in appendix.

4.4. Contribution of HE-DA

The results presented in Table 5 clearly demonstrate the superiority of our high energy-based data augmentation (HE-DA) method over using the entire dataset. Despite applying HE-DA to only 20% of the data (i.e., $r = 0.2$), we achieve performance comparable to applying data augmentation to the entire dataset. Furthermore, when HE-DA is applied to 40-50% of the data, we observe substantial performance improvements ranging from 0.3 to 0.7, providing strong evidence of the effectiveness of our approach.

Figure 2 represent the performance variations according to the sample types. The experiments clearly demonstrate that using exclusively high energy samples results in higher performance compared to using low energy or a combination of both samples. When a balanced mix of low energy and high

Teacher	WRN-40-2	ResNet-56	ResNet-32x4	VGG 13	VGG 13	ResNet-32x4
Student	WRN-16-2	ResNet-20	ResNet-8x4	VGG 8	MobileNetV2	ShuffleNetV2
KD	74.92	70.66	73.33	72.98	67.37	74.45
KD+CutMix (100%)	75.34	70.77	74.91	74.16	<u>68.79</u>	76.61
HE-DA (20%)	75.27	70.90	74.84	74.04	68.06	76.57
HE-DA (30%)	75.54	71.15	74.85	74.17	68.62	76.87
HE-DA (40%)	<u>75.72</u>	71.43	<u>75.13</u>	<u>74.42</u>	68.69	<u>77.16</u>
HE-DA (50%)	75.95	<u>71.26</u>	75.22	74.54	69.13	77.32
Δ	+0.61	+0.66	+0.31	+0.38	+0.34	+0.71

Table 5: Performance assessed when applying High Energy-based Data Augmentation (HE-DA) to the CIFAR-100 test sets using teacher and student models with both identical and distinct architectures.

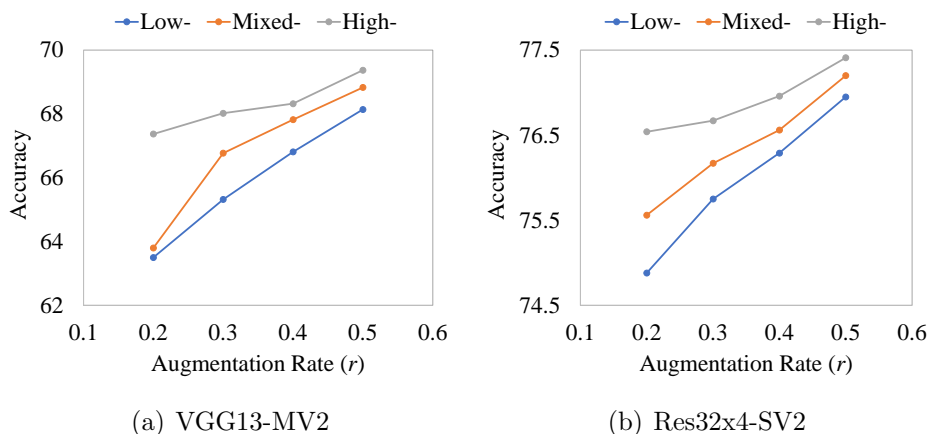


Figure 2: Performance variations according to the sample types: low, high, and mixed energy. (a): VGG13/MobileNetV2, (b): ResNet32x4/ShuffleNetV2

energy data is employed (50/50), the performance falls between the two extremes, with using only high energy data yielding superior results and using only low energy data leading to lower performance. These results indicate that decreasing the proportion of low energy data positively affects performance. The reason behind this could be the learning model’s proficiency in grasping low energy samples. Consequently, adding further augmentation might lead to confusion in these samples, impeding the learning process of the model. Thus, to achieve optimal performance, it is suggested to decrease the quantity of low energy samples and rely solely on high energy samples.

Furthermore, it is worth noting that the accuracy of high energy results remains relatively stable, regardless of the variation in augmentation rates

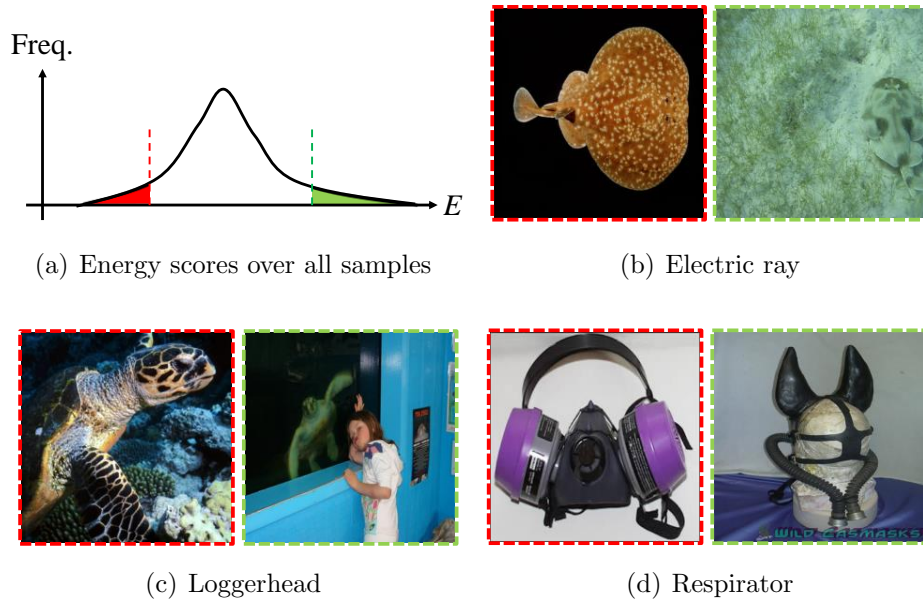


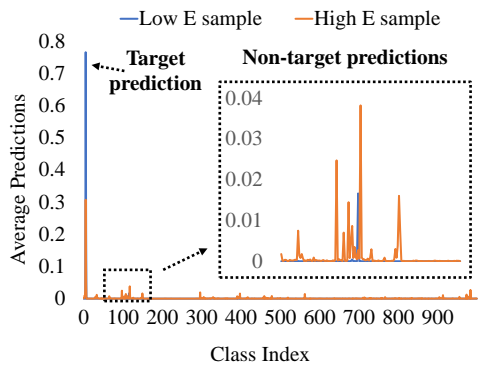
Figure 3: ImageNet samples categorized according to their energy scores obtained from ResNet32x4. The red boxes belong to the certain images and have low energy scores, accurately representing their assigned labels. The green boxes are relative to the uncertain images and have high energy scores, not clearly reflecting their assigned labels.

that determines the level of data enrichment. In other words, when dealing with high energy data, augmenting 10% to 20% of the dataset shows no significant difference compared to augmenting 40% to 50% of the data. However, for low energy data, augmenting 10% to 20% of the dataset may result in lower performance compared to having no augmentation at all. This finding suggests that the accuracy of high energy data is not significantly affected by changes in the augmentation rate. This characteristic can be particularly valuable in scenarios where computational resource is severely limited.

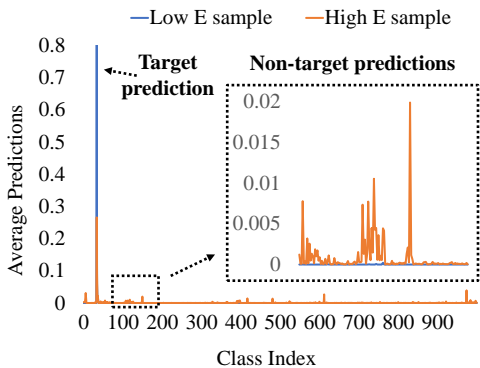
4.5. Low and High energy Samples

To validate the insights gained from the energy scores, it is valuable to visualize the images belonging to both the low energy and high energy.

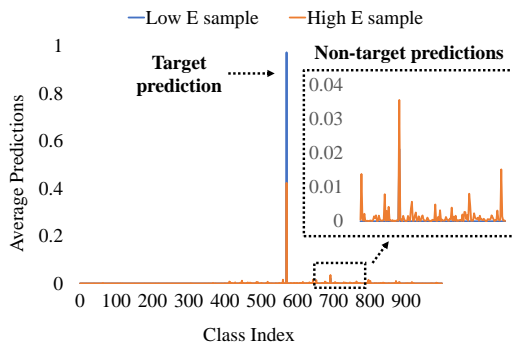
Figure 3 illustrates the categorization of ImageNet based on the energy score of each image, dividing them into categories of low energy and high energy samples. The red boxes depicts images with low energy scores, effectively representing their respective classes. We have denoted this category as



(a) Electric ray



(b) Loggerhead



(c) Respirator

Figure 4: Average predictions for particular classes with low energy (blue line) and high energy (red line) samples. Low energy samples exhibit high confidence scores and lack substantial dark knowledge, whereas high energy samples display low confidence scores and have inordinate knowledge.

'certain images'. On the other hand, the green boxes displays images with high energy scores, indicating either a confused label or a mixture of different objects. These images have been designated as 'uncertain images'.

Figure 4 demonstrates the average predictions for 'certain' and 'uncertain' images. Certain images exhibit high confidence scores and possess insufficient knowledge about non-target predictions, while uncertain images showcase low confidence scores and a relatively uniform distribution. It's worth noting that the predictions presented in Figure 4 support the classification of each image as either certain or uncertain. These findings align with prior research (Liu et al. (2020b)) that higher energy levels are associated with out-of-distribution (OOD) data. An important difference is that we categorize low energy and high energy data within the same dataset based on our criteria. Additional images are available in appendix.

As a result, it is resonable to utilize higher temperature values for low energy samples to create smoother predictions and lower temperature values for high energy samples to achieve sharper predictions during the distillation process. This ensures that the teacher model optimally transfers its knowledge to the student model.

4.6. Computational Costs

Table 6 displays the computational cost in relation to the percentage of DA applied. This refers to the learning time per epoch on the CIFAR-100 datasets. As previously mentioned, we observe that applying DA to the entire dataset results in a 33.26% increase in computational cost. When applying DA to 40-50% of the dataset (which produces the peak performance of our methodology), we notice an increase in computational expenses by only 8.78-14.17%. These results demonstrate that our approach excels not only in terms of performance but also in terms of efficiency. Our computing infrastructure used for this experiment is introduced in appendix.

r	0.1	0.2	0.3	0.4	0.5	1.0
% \uparrow	0.0%	3.94%	5.52%	8.78%	14.17%	33.26%

Table 6: Computational costs are measured according to the rate at which Data Augmentation (DA) is applied. The percentage rise is computed based on the value of $r = 0.1$.

4.7. Long-tailed Dataset

Table 7 shows the experimental results using the CIFAR-100 long-tail (LT) dataset. CIFAR-100-LT and CIFAR-100 were used for training and

testing, respectively. Our experiments were performed with 4 different architecture pairs. In the case of the long-tail type, exponential decay was used, and an imbalance factor of 0.5 was applied. More detailed experimental parameters are provided in appendix. Our method outperforms the state-of-the-art DKD and ReviewKD methods. This is because we further optimized the knowledge distillation by applying different temperatures for low energy and high energy samples based on their energy score. These findings indicate that our approach remains resilient when dealing with challenging dataset. The results were also evident in our experiments on the ImageNet dataset, which comprises a significant disparity in the number of samples among classes.

Teacher	Res32x4	VGG 13	VGG 13	Res32x4
Student	Res8x4	VGG 8	MV2	SV2
KD	72.51	71.59	65.19	72.93
DKD	73.60	73.25	66.73	74.09
ReviewKD	73.42	73.02	66.36	74.11
Energy KD	73.97	73.73	67.08	74.61

Table 7: Top-1 accuracy (%) on the CIFAR-100-LT datasets, employing both identical and distinct architectures for teacher and student models.

5. Conclusions

In this paper, we present a new perspective that considers the energy score of a sample, which has not been utilized in traditional KD approaches. In this approach, we classify datasets into low energy and high energy samples based on their energy scores, and apply higher temperatures to low energy samples and lower temperatures to high energy samples. Compared to traditional logit-based and feature-based methods, energy-based KD (EnergyKD) performs better on a variety of datasets. In particular, on the challenging datasets CIFAR-100-LT and ImageNet, EnergyKD shows significant performance gains, proving that it is a more effective method on real-world datasets. Furthermore, by applying HE-DA, it further improves performance and is much more efficient in terms of computational cost. We hope that our framework, which provides a new perspective on considering energy score of samples in KD, will be utilized in future work.

References

- Ackley, D.H., Hinton, G.E., Sejnowski, T.J., 1985. A learning algorithm for boltzmann machines. *Cognitive science* 9, 147–169.
- Ahn, S., Hu, S.X., Damianou, A., Lawrence, N.D., Dai, Z., 2019. Variational information distillation for knowledge transfer, in: *Proceedings of the IEEE/CVF Conference on Computer Vision and Pattern Recognition*, pp. 9163–9171.
- Chen, P., Liu, S., Zhao, H., Jia, J., 2021a. Distilling knowledge via knowledge review, in: *Proceedings of the IEEE/CVF Conference on Computer Vision and Pattern Recognition*, pp. 5008–5017.
- Chen, P., Liu, S., Zhao, H., Jia, J., 2021b. Distilling knowledge via knowledge review, in: *CVPR*.
- Cho, J.H., Hariharan, B., 2019. On the efficacy of knowledge distillation, in: *ICCV*.
- Furlanello, T., Lipton, Z., Tschannen, M., Itti, L., Anandkumar, A., 2018. Born again neural networks, in: *ICML*.
- Gou, J., Yu, B., Maybank, S.J., Tao, D., 2021. Knowledge distillation: A survey. *International Journal of Computer Vision* 129, 1789–1819.
- Grathwohl, W., Wang, K.C., Jacobsen, J.H., Duvenaud, D., Norouzi, M., Swersky, K., 2019. Your classifier is secretly an energy based model and you should treat it like one. *arXiv preprint arXiv:1912.03263* .
- He, K., Gkioxari, G., Dollár, P., Girshick, R., 2017. Mask r-cnn, in: *Proceedings of the IEEE international conference on computer vision*, pp. 2961–2969.
- He, K., Zhang, X., Ren, S., Sun, J., 2016a. Deep residual learning for image recognition, in: *Proceedings of the IEEE conference on computer vision and pattern recognition*, pp. 770–778.
- He, K., Zhang, X., Ren, S., Sun, J., 2016b. Deep residual learning for image recognition, in: *CVPR*.

- Heo, B., Kim, J., Yun, S., Park, H., Kwak, N., Choi, J.Y., 2019a. A comprehensive overhaul of feature distillation, in: ICCV.
- Heo, B., Kim, J., Yun, S., Park, H., Kwak, N., Choi, J.Y., 2019b. A comprehensive overhaul of feature distillation, in: Proceedings of the IEEE International Conference on Computer Vision, pp. 1921–1930.
- Heo, B., Lee, M., Yun, S., Choi, J.Y., 2019c. Knowledge transfer via distillation of activation boundaries formed by hidden neurons, in: AAAI.
- Hinton, G., Vinyals, O., Dean, J., 2015. Distilling the knowledge in a neural network. arXiv preprint arXiv:1503.02531 .
- Huang, Z., Wang, N., 2017. Like what you like: Knowledge distill via neuron selectivity transfer. arXiv:1707.01219 .
- Kim, J., Park, S., Kwak, N., 2018. Paraphrasing complex network: Network compression via factor transfer, in: NeurIPS.
- Krizhevsky, A., Hinton, G., et al., 2009. Learning multiple layers of features from tiny images .
- LeCun, Y., Chopra, S., Hadsell, R., Ranzato, M., Huang, F., 2006. A tutorial on energy-based learning. Predicting structured data 1.
- Li, X.C., Fan, W.S., Song, S., Li, Y., Yunfeng, S., Zhan, D.C., et al., 2022. Asymmetric temperature scaling makes larger networks teach well again. Advances in Neural Information Processing Systems 35, 3830–3842.
- Liu, J., Zhuang, B., Zhuang, Z., Guo, Y., Huang, J., Zhu, J., Tan, M., 2021. Discrimination-aware network pruning for deep model compression. IEEE Transactions on Pattern Analysis and Machine Intelligence 44, 4035–4051.
- Liu, W., Wang, X., Owens, J., Li, Y., 2020a. Energy-based out-of-distribution detection. Advances in neural information processing systems 33, 21464–21475.
- Liu, W., Wang, X., Owens, J., Li, Y., 2020b. Energy-based out-of-distribution detection. Advances in neural information processing systems 33, 21464–21475.

- Long, J., Shelhamer, E., Darrell, T., 2015. Fully convolutional networks for semantic segmentation, in: Proceedings of the IEEE conference on computer vision and pattern recognition, pp. 3431–3440.
- Ma, N., Zhang, X., Zheng, H.T., Sun, J., 2018a. Shufflenet v2: Practical guidelines for efficient cnn architecture design, in: Proceedings of the European conference on computer vision (ECCV), pp. 116–131.
- Ma, N., Zhang, X., Zheng, H.T., Sun, J., 2018b. Shufflenet V2: Practical guidelines for efficient cnn architecture design, in: ECCV.
- Mirzadeh, S.I., Farajtabar, M., Li, A., Levine, N., Matsukawa, A., Ghasemzadeh, H., 2020. Improved knowledge distillation via teacher assistant, in: AAAI.
- Park, W., Kim, D., Lu, Y., Cho, M., 2019a. Relational knowledge distillation, in: CVPR.
- Park, W., Kim, D., Lu, Y., Cho, M., 2019b. Relational knowledge distillation, in: Proceedings of the IEEE/CVF Conference on Computer Vision and Pattern Recognition, pp. 3967–3976.
- Ranzato, M., Boureau, Y.L., Chopra, S., LeCun, Y., 2007. A unified energy-based framework for unsupervised learning, in: Artificial Intelligence and Statistics, PMLR. pp. 371–379.
- Ranzato, M., Poultney, C., Chopra, S., Cun, Y., 2006. Efficient learning of sparse representations with an energy-based model. Advances in neural information processing systems 19.
- Ren, S., He, K., Girshick, R., Sun, J., 2015. Faster r-cnn: Towards real-time object detection with region proposal networks. Advances in neural information processing systems 28.
- Romero, A., Ballas, N., Kahou, S.E., Chassang, A., Gatta, C., Bengio, Y., 2014. Fitnets: Hints for thin deep nets. arXiv preprint arXiv:1412.6550 .
- Russakovsky, O., Deng, J., Su, H., Krause, J., Satheesh, S., Ma, S., Huang, Z., Karpathy, A., Khosla, A., Bernstein, M., et al., 2015. Imagenet large scale visual recognition challenge. International journal of computer vision 115, 211–252.

- Salakhutdinov, R., Larochelle, H., 2010. Efficient learning of deep boltzmann machines, in: Proceedings of the thirteenth international conference on artificial intelligence and statistics, JMLR Workshop and Conference Proceedings. pp. 693–700.
- Sandler, M., Howard, A., Zhu, M., Zhmoginov, A., Chen, L.C., 2018. MobilenetV2: Inverted residuals and linear bottlenecks, in: CVPR.
- Tian, Y., Krishnan, D., Isola, P., 2019. Contrastive representation distillation. arXiv preprint arXiv:1910.10699 .
- Xie, J., Lu, Y., Gao, R., Zhu, S.C., Wu, Y.N., 2018a. Cooperative training of descriptor and generator networks. IEEE transactions on pattern analysis and machine intelligence 42, 27–45.
- Xie, J., Zheng, Z., Gao, R., Wang, W., Zhu, S.C., Wu, Y.N., 2018b. Learning descriptor networks for 3d shape synthesis and analysis, in: Proceedings of the IEEE conference on computer vision and pattern recognition, pp. 8629–8638.
- Xie, J., Zhu, S.C., Wu, Y.N., 2019. Learning energy-based spatial-temporal generative convnets for dynamic patterns. IEEE transactions on pattern analysis and machine intelligence 43, 516–531.
- Yang, C., Xie, L., Su, C., Yuille, A.L., 2019. Snapshot distillation: Teacher-student optimization in one generation, in: CVPR.
- Yun, S., Han, D., Oh, S.J., Chun, S., Choe, J., Yoo, Y., 2019. Cutmix: Regularization strategy to train strong classifiers with localizable features, in: Proceedings of the IEEE/CVF international conference on computer vision, pp. 6023–6032.
- Zagoruyko, S., Komodakis, N., 2016a. Paying more attention to attention: Improving the performance of convolutional neural networks via attention transfer. arXiv preprint arXiv:1612.03928 .
- Zagoruyko, S., Komodakis, N., 2016b. Wide residual networks, in: BMVC.
- Zhang, H., Cisse, M., Dauphin, Y.N., Lopez-Paz, D., 2017. mixup: Beyond empirical risk minimization. arXiv preprint arXiv:1710.09412 .

- Zhang, Y., Xiang, T., Hospedales, T.M., Lu, H., 2018. Deep mutual learning, in: CVPR.
- Zhao, B., Cui, Q., Song, R., Qiu, Y., Liang, J., 2022. Decoupled knowledge distillation, in: Proceedings of the IEEE/CVF Conference on computer vision and pattern recognition, pp. 11953–11962.
- Zhao, H., Shi, J., Qi, X., Wang, X., Jia, J., 2017. Pyramid scene parsing network, in: Proceedings of the IEEE conference on computer vision and pattern recognition, pp. 2881–2890.
- Zhao, J., Mathieu, M., LeCun, Y., 2016. Energy-based generative adversarial network. arXiv preprint arXiv:1609.03126 .
- Zhou, Y., Moosavi-Dezfooli, S.M., Cheung, N.M., Frossard, P., 2018. Adaptive quantization for deep neural network, in: Proceedings of the AAAI Conference on Artificial Intelligence.